

Swift/XRT view on S5 0716+714 during a flare

A. Wierzholska^{1,2*} and H. Siejkowski³

¹*Institute of Nuclear Physics, Polish Academy of Sciences, ul. Radzikowskiego 152, 31-342 Kraków, Poland*

²*Landessternwarte, Universität Heidelberg, Königstuhl, D 69117 Heidelberg, Germany*

³*AGH University of Science and Technology, ACC Cyfronet AGH, ul. Nawojki 11, PO Box 386, 30-950, Kraków 23, Poland*

Accepted 2015 May 13 Received 2015 May 9; in original form 2015 March 29

ABSTRACT

The blazar S5 0716+714 has been monitored in its flaring state between 2015 January 19 and February 22 with *Swift*/XRT. During this period an exceptional flux level was observed in the X-ray range as well as in the other wavelengths, e.g. optical, near infrared and very high energy γ rays. Here, we report X-ray observations of S5 0716+714 carried out during the outburst. The observed X-ray spectra, well described with broken power-law model, disentangle both synchrotron and inverse Compton components. The break energy shifts towards higher energies with increasing flux, revealing the dominance of synchrotron radiation in the X-ray spectrum observed. We also report spectrum softening with increasing flux. During the recent flare, significant temporal intranight variability is observed in the X-ray range.

Key words: galaxies: active – BL Lacertae objects: general, BL Lacertae objects: individual: S5 0716+714 – X-rays: general.

1 INTRODUCTION

Blazars are the most extreme Active Galactic Nuclei with non-thermal emission observed from the jet visible at small angle to the observer's line of sight (e.g., Begelman et al. 1984). This group of sources includes BL Lacertae type objects as well as quasar-type blazars known as flat-spectrum radio quasars (FSRQs), high-polarization quasars (HPQs) or optically violent variables (OVVs), depending on the properties used for classification i.e.: radio spectral index, optical polarization or optical variability, respectively. Broad-band emission is observed from radio frequencies up to high energy or very high energy gamma rays (e.g., Wagner 2009; Vercellone et al. 2011; Abramowski & et al. HESS Collaboration, H). The characteristic feature of blazars is their variability, manifested in all wavelengths, with different variability time scales down to hours or even minutes in the most extreme cases (e.g. Wagner & Witzel 1995; Aharonian et al. 2007; Gopal-Krishna et al. 2011; Saito et al. 2013; Liao & Bai 2015).

The spectral energy distribution (SED), in ν - νF_ν representation has a characteristic double-humped structure. This curvature of SED has been widely discussed in the literature, considering both leptonic and hadronic scenarios as a possible explanation (for review see e.g. Böttcher et al. 2013). In the most popular, so-called Synchrotron-self-Compton scenario, the first bump is attributed to the synchrotron radiation originating from relativistic electrons

from the jet, while the second is produced in inverse Compton process, involving the same population of electrons and jet synchrotron photons. The location of peaks in SED allows to subdivide sources into high-energy, intermediate-energy and low-energy peaked objects: HBL, IBL and LBL, respectively (see, e.g., Abdo et al. 2010).

S5 0716+714 is a very bright (e.g. Aliu et al. 2012) IBL type blazar located at $z = 0.31$ (Donato et al. 2001). Several multi-frequency campaigns have targeted this source (e.g. Dai et al. 2013; Liao et al. 2014; Wu et al. 2014). The objects was also frequently monitored in X-ray range with different instruments reporting both spectral and temporal variability (e.g. Wagner 1992; Cappi et al. 1994; Liao et al. 2014). It is worth mentioning here that X-ray observations of S5 0716+714 revealed both synchrotron and inverse Compton components manifested in this domain (Cappi et al. 1994; Giommi et al. 1999; Tagliaferri et al. 2003; Donato et al. 2005; Ferrero et al. 2006).

2 OBSERVATIONS AND DATA ANALYSIS

The *Swift* mission (Gehrels et al. 2004) is a multi-wavelength space observatory equipped with following detectors: the Burst Alert Telescope (BAT, Barthelmy et al. 2005), X-ray Telescope (XRT, Burrows et al. 2005) and Ultraviolet/Optical Telescope (UVOT, Roming et al. 2005). Here, we study X-ray observations in the energy range of 0.3-10 keV obtained with *Swift*/XRT. Since April 2005 S5 0716+714 has been monitored in several pointed observations, both in pho-

* E-mail: alicja.wierzholska@ifj.edu.pl

ton counting (PC) and windowed timing (WT) modes. In this study, we focus on the flare observed during the period of 2015 January 19–February 22. The total exposure of the *Swift*/XRT observations studied (IDs 00035009146–00035009202) is 152 ks. Data were analysed using version 6.16 of the HEASOFT package¹ with CALDB v.20140120 following the standard procedure `xrtpipeline`. Spectral analysis is performed in the energy range of 0.3–10 keV with the latest version of XSPEC package (version 12.8.2). All data are binned to have a minimum of 30 counts per bin. A single power-law model and also a broken power-law one are tested, both with hydrogen Galactic absorption $N_H = 3.22 \cdot 10^{20} \text{ cm}^{-2}$ (Kalberla et al. 2005) fixed as a frozen parameter.

3 SPECTRAL AND TEMPORAL VARIABILITY

The long-term light curve of S5 0716+714 and a zoom of the flare studied are presented in Fig. 1 and in the upper panel of Fig. 2, respectively. During the outburst, significant variability of the source is observed. The maximum flux during this flare is about $1.8 \text{ counts s}^{-1}$. It is worth mentioning here that the flare reaches the highest flux level ever observed for S5 0716+714 with *Swift*/XRT and it is best sampled outburst for this source with this instrument. Data collected during the flare (separately in PC and WT mode) were fitted with single power-law and broken power-law models, in both cases with Galactic absorption. A comparison of the fit parameters for both models, as well as values of the χ^2 statistic, is presented in Table 1. A single power-law model with a frozen value of N_H yields worse fit to data.

Thus, the broken power-law model is the preferable description of the spectrum for S5 0716+714. The higher value of χ^2_{red} in WT mode was expected, since only the PC mode retains full imaging and spectroscopic resolution. In the spectra derived, in PC mode as well as in WT mode, an upturn for broken power-law model is revealed at about 4–5 keV. Fig. 3 shows an example of broken power-law fit to the data in the case of all observations of the recent flare in PC mode. The corresponding spectral energy distribution with an upturn point of 3.98 keV is presented in the bottom panel of Fig. 3.

In order to investigate spectral variability in greater detail, the single power-law and broken power-law models were also tested for four shorter intervals of observations, marked in Fig. 2 and defined in Table 2. The intervals were optimized to have good enough statistics and observed either in PC or WT mode. The fit parameters for models as well as values of χ^2 statistics are collected in Table 1. For all the intervals both power-law as well as broken power-law models were tested using *F*-test (e.g. Bevington & Robinson 2003), resulting in probability value for predominance of power-law model of 6, 0.2, 6.6 and < 1 per cent for intervals (1), (2), (3) and (4), respectively. Hence, the favourable model of the spectra for these four intervals is a broken power-law disentangling both synchrotron and inverse Compton

Table 2. Selected intervals for detailed spectral studies. The following columns present: the number of the interval or information about data used; the observation ID – 00035009000; the total exposure; the observation mode.

Interval	Observation IDs	Exposure [ks]	Mode
(1)	147–153	11.1	PC
(2)	154–161	23.3	PC
(3)	169–173	19.3	WT
(4)	175–188	77.4	WT
all PC	147–202	102.9	PC
all WT	147–202	49.1	WT

components in the X-ray regime. The break energy shifts towards higher values with higher flux levels.

Fig. 2 shows light curves in five different energy bands, i.e.: 0.3–10, 0.3–5, 5–10, 0.3–1 and 1–10 keV. As was shown in the case of the integrated spectrum for S5 0716+714 the upturn is located at about 5 keV. Hence, the light curves in the energy bands of 0.3–5 and 5–10 keV (the second and the third panels in Fig. 2) compare synchrotron and inverse Compton emission, respectively. The light curve in 0.3–5 keV band follows the one in 0.3–10 keV energy range. The low statistics of inverse Compton photons cause a worse description of this part of the spectrum (see Table 1). This also does not allow us either to claim or to exclude variability of the inverse Compton component. The flux changes in different energy bands at 0.3–10, 0.3–5, 0.3–1 and 1–10 keV, reveal similar variability patterns and seem to be correlated.

The comparison of the hardness ratios for the two cases defined as: $HR_5 = F(5\text{--}10 \text{ keV})/F(0.3\text{--}5 \text{ keV})$ and $HR_1 = F(1\text{--}10 \text{ keV})/F(0.3\text{--}1 \text{ keV})$, with the source intensity $F(0.3\text{--}10 \text{ keV})$ (see Fig. 4) shows evidence in both cases for spectral steepening with increasing intensity. We denote the flux count rate for a given energy range as $F(E_{min}, E_{max})$. The comparison reveals an anticorrelation in the hardness-ratio-intensity plot. This behaviour has been found in several IBL-type blazars (e.g. Ferrero et al. 2006), while in the case of HBL objects harder-when-brighter chromatism is observed (e.g. Takahashi et al. 1996, 1999). This effect, described by Padovani & Giommi (1996), is explained in the context of the synchrotron variability, which steepens the overall X-ray spectrum with increasing total flux (e.g. Giommi et al. 1999; Ferrero et al. 2006; Foschini et al. 2006).

The recent intensive monitoring of S5 0716+714 results in eight nights during which the exposure of the observations is larger than 6 ks. For these nights, detailed light curves (with snapshot-wise bins) are presented in Fig. 5. The relatively high flux observed in each case gives a perfect possibility of studying intranight variability in the X-ray regime. In all the cases significant variability is detected, fitting with a constant to data points results in a value of χ^2_{red} of at least 2. The largest intranight variability is observed on MJD 57054 with χ^2_{red} equal to 16.

4 SUMMARY AND CONCLUSIONS

Swift/XRT observations of S5 0716+714 performed during the period of 2015 January 19–February 22 show significant brightness increase of the source. S5 0716+714 is known to

¹ <http://heasarc.gsfc.nasa.gov/docs/software/lheasoft>

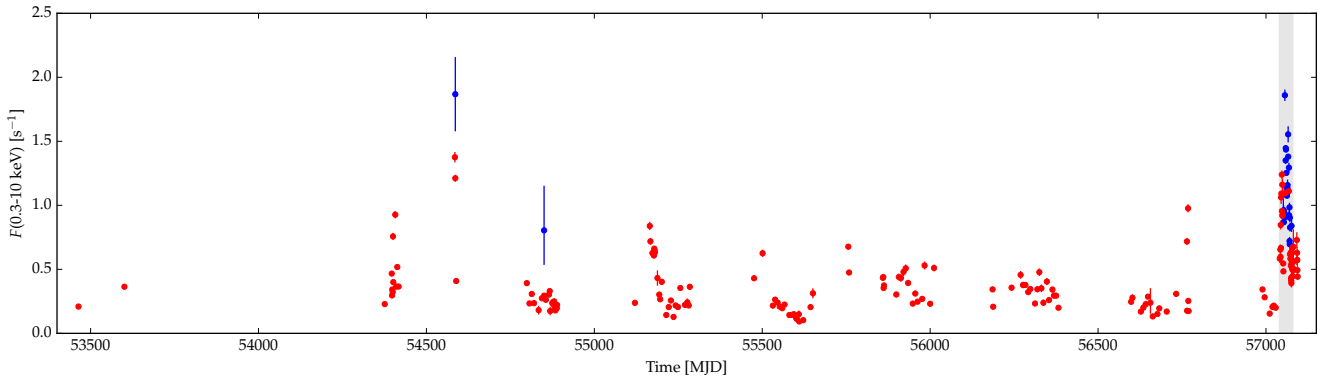


Figure 1. *Swift*/XRT long-term light curve of S5 0716+714 including monitoring of the blazar since April 2005 in the energy range of 0.3-10 keV. Grey shaded area indicates flare interval discussed in this paper. Observations taken in PC mode and WT mode are marked in red and blue, respectively.

Table 1. The parameters for power-law and broken power-law fits to the data. The following columns give: the number of interval or information about data used; the normalization, the photon indices, the break energy and the reduced χ^2 value for broken power-law fit; the normalization, the photon index and the reduced χ^2 value for power-law fit. Normalizations N_{br} and N_{po} are given in $10^{-3} \text{ cm}^{-2} \text{ s}^{-1} \text{ keV}^{-1}$, while break energy is expressed in keV.

Interval	N_{br}	γ_1	γ_2	E_{br}	$\chi^2_{red,br}(\text{d.o.f.})$	N_{po}	γ	$\chi^2_{red,po}(\text{d.o.f.})$
(1)	3.913 ± 0.061	2.375 ± 0.028	1.08 ± 0.10	4.68 ± 0.74	1.111(214)	3.927 ± 0.061	2.353 ± 0.025	1.130(216)
(2)	6.466 ± 0.061	2.541 ± 0.015	0.20 ± 0.80	5.75 ± 0.50	0.957(288)	6.479 ± 0.061	2.532 ± 0.015	0.994(290)
(3)	5.184 ± 0.054	2.391 ± 0.018	1.27 ± 0.42	5.10 ± 0.50	1.294(263)	5.187 ± 0.054	2.380 ± 0.018	1.311(265)
(4)	7.657 ± 0.029	2.663 ± 0.068	0.10 ± 0.10	5.10 ± 0.50	2.473(268)	7.688 ± 0.029	2.646 ± 0.066	2.862(470)
all PC	5.125 ± 0.036	2.447 ± 0.012	1.73 ± 0.20	3.98 ± 0.38	1.177(390)	5.150 ± 0.035	2.425 ± 0.011	1.237(392)
all WT	7.050 ± 0.025	2.622 ± 0.062	0.10 ± 0.10	5.20 ± 0.40	2.663(514)	7.072 ± 0.025	2.606 ± 0.061	3.003(516)

be a very variable object, and not only in the X-ray range (e.g. Wagner 1992; Cappi et al. 1994; Tagliaferri et al. 2003; Donato et al. 2005; Liao et al. 2014). The elevated flux of the source during the most recent flare was reported in different wavelengths e.g. optical (Bachev et al. 2015; Bachev & Strigachev 2015; Spiridonova et al. 2015), near-infrared (Carrasco et al. 2015), and very high energy gamma rays (Mirzoyan 2015). During the period observed, the flaring activity was not detected in GeV monitoring with *Fermi* Large Area Telescope².

Since the monitoring programmes mentioned do not provide publicly available light curves, we are not able to judge whether the shape of the flare is similar at other wavelengths or not. However, we note here, that the mentioned Astronomer's Telegrams report an exceptional behaviour of S5 0716+714 starting from January 16. The *Swift*/XRT monitoring of the blazar started on January 19, but the highest flux level observed was detected in the X-ray regime a few days later.

Previous studies of the source in X-ray domain revealed both synchrotron and inverse Compton components in the X-ray range, with break energy in the range of 1.5-3.0 keV (Tagliaferri et al. 2003; Donato et al. 2005; Ferrero et al. 2006; Foschini et al. 2006). We note here that observations mentioned were mostly performed in the quiescence state of the blazar. Ferrero et al. (2006) studied changes of the break energy in broken power-law spectral fit for different

flux levels. The authors have shown that, during the elevated flux-level period, the crossing point is shifted to a higher energy of about 5 keV, while for the lower flux states the upturn occurs at about 2 keV.

In our studies, we found that the X-ray variable spectrum of S5 0716+714 is well described with broken power-law model. This description is consistent with synchrotron cooling processes associated with a single emitting component. The lack of any significant spectral variability also confirms that there is no need of any additional emitting component. The break energy in broken power-law description shifts to higher values with increasing flux level. We found that most of the X-ray emission is observed in the energy range of 0.3-5 keV. Furthermore, we found that source follows the softer-when-brighter trend typical for IBL-type objects (e.g. Ferrero et al. 2006).

The temporal variability studies of S5 0716+714 have revealed significant intranight variability in the X-ray regime. Previously, in this blazar, such feature has been observed mainly in the optical regime (e.g. Montagni et al. 2006; Bogdan et al. 2015).

ACKNOWLEDGEMENTS

We thank the Swift PI, Neil Gehrels, for accepting our request for ToO observations of S5 0716+714 with *Swift*/XRT. A.W. acknowledges support by Polish Ministry of Science and Higher Education in Mobility Plus Program and Polish

² http://fermi.gsfc.nasa.gov/ssc/data/access/lat/msl_lc/

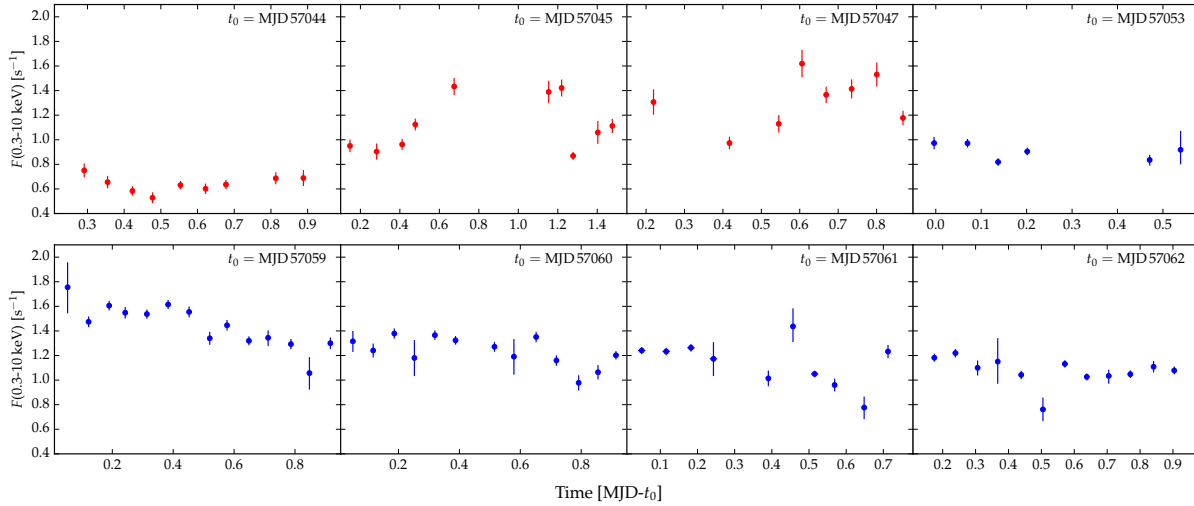


Figure 5. Intra-night variability visible during 8 selected nights of the recent flare. Observations taken in PC mode and WT mode are marked in red and blue, respectively. Modified Julian Date of each observation night is given in right top corner in each plot and the x-axis shows fractional part of the day.

National Science Center for supporting this work through grant DEC-2011/03/N/ST9/01867. This research was supported in part by PLGrid Infrastructure.

REFERENCES

- Abdo A. A. et al., 2010, *ApJ*, 716, 30
- Abramowski A., et al. (HESS Collaboration), 2013, *A&A*, 559, A136
- Abramowski A., et al. (HESS Collaboration), 2014, *A&A*, 571, A39
- Aharonian F. et al., 2007, *ApJ*, 664, L71
- Aliu E. et al., 2012, *ApJ*, 750, 94
- Bachev R., Spassov B., Boeva S., 2015, *The Astronomer's Telegram*, 6944, 1
- Bachev R., Strigachev A., 2015, *The Astronomer's Telegram*, 6957, 1
- Barthelmy S. D. et al., 2005, *Space Sci. Rev.*, 120, 143
- Begelman M. C., Blandford R. D., Rees M. J., 1984, *Reviews of Modern Physics*, 56, 255
- Bevington P., Robinson D., 2003, *Data reduction and error analysis for the physical sciences*, McGraw-Hill Higher Education, McGraw-Hill, Boston, MA
- Bogdan D., Alexandru M., Raluca M. G., 2015, *Research in Astronomy and Astrophysics*, 15, 327
- Böttcher M., Reimer A., Sweeney K., Prakash A., 2013, *ApJ*, 768, 54
- Burrows D. N. et al., 2005, *Space Sci. Rev.*, 120, 165
- Cappi M., Comastri A., Molendi S., Palumbo G. G. C., Della Ceca R., Maccacaro T., 1994, *MNRAS*, 271, 438
- Carrasco L., Porras A., Recillas E., Leon-Tavares J., Chavushyan V., Carraminana A., 2015, *The Astronomer's Telegram*, 6902, 1
- Dai Y., Wu J., Zhu Z.-H., Zhou X., Ma J., Yuan Q., Wang L., 2013, *ApJS*, 204, 22
- Donato D., Ghisellini G., Tagliaferri G., Fossati G., 2001, *A&A*, 375, 739
- Donato D., Sambruna R. M., Gliozzi M., 2005, *A&A*, 433, 1163
- Ferrero E., Wagner S. J., Emmanoulopoulos D., Ostorero L., 2006, *A&A*, 457, 133
- Foschini L. et al., 2006, *A&A*, 455, 871
- Gehrels N. et al., 2004, *ApJ*, 611, 1005
- Giommi P. et al., 1999, *A&A*, 351, 59
- Gopal-Krishna, Goyal A., Joshi S., Karthick C., Sagar R., Wiita P. J., Anupama G. C., Sahu D. K., 2011, *MNRAS*, 416, 101
- Kalberla P. M. W., Burton W. B., Hartmann D., Arnal E. M., Bajaja E., Morras R., Pöppel W. G. L., 2005, *A&A*, 440, 775
- Liao N. H., Bai J. M., 2015, *New A*, 34, 134
- Liao N. H., Bai J. M., Liu H. T., Weng S. S., Chen L., Li F., 2014, *ApJ*, 783, 83
- Mirzoyan R., 2015, *The Astronomer's Telegram*, 6999, 1
- Montagni F., Maselli A., Massaro E., Nesci R., Sclavi S., Maesano M., 2006, *A&A*, 451, 435
- Padovani P., Giommi P., 1996, *MNRAS*, 279, 526
- Roming P. W. A. et al., 2005, *Space Sci. Rev.*, 120, 95
- Saito S., Stawarz L., Tanaka Y. T., Takahashi T., Madejski G., D'Ammando F., 2013, *ApJ*, 766, L11
- Spiridonova O. I., Vlasjuk V. V., Moskvitin A. S., Bychkova V. S., 2015, *The Astronomer's Telegram*, 7004, 1
- Tagliaferri G. et al., 2003, *A&A*, 400, 477
- Takahashi T., Madejski G., Kubo H., 1999, *Astroparticle Physics*, 11, 177
- Takahashi T. et al., 1996, *ApJ*, 470, L89
- Vercellone S. et al., 2011, *ApJ*, 736, L38
- Wagner S., 2009, in *Astrophysics with All-Sky X-Ray Observations*. RIKEN, and JAXA Suzuki Umetaro Hall, RIKEN Wako, Saitama, Japan, Kawai N., Mihara T., Kohama M., Suzuki M., eds., p. 186
- Wagner S. J., 1992, in *X-ray Emission from Active Galactic Nuclei and the Cosmic X-ray Background*, Max-Planck-Institut für Extraterrestrische Physik, Garching bei München, Germany, Brinkmann W., Truemper J., eds., pp. 97–102

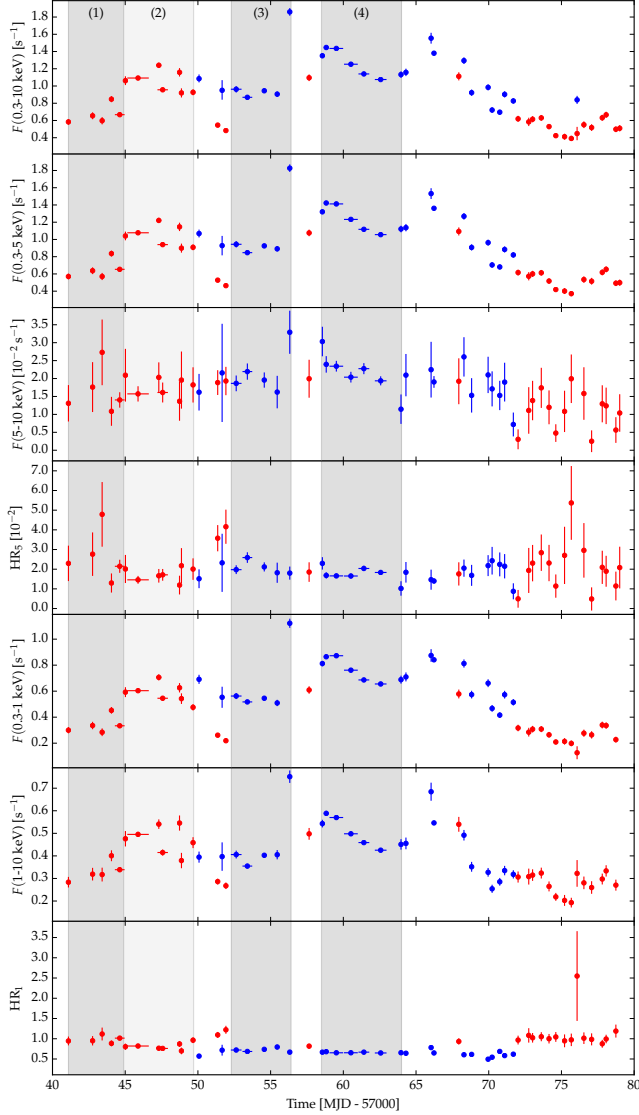


Figure 2. The light curve of S5 0716+714 presenting *Swift*/XRT observations taken during the recent flare. The following panels show light curve in the energy bands of: 0.3-10 keV, 0.3-5 keV, 5-10 keV, 0.3-1 keV, 1-10 keV and the corresponding hardness ratios. The intervals selected for spectral analysis discussed in Sec. 3 are marked with grey areas. Observations taken in PC mode and WT mode are denoted in red and blue, respectively.

Wagner S. J., Witzel A., 1995, ARA&A, 33, 163
Wu J., Dai Y., Zhou X., Ma J., 2014, JA&A

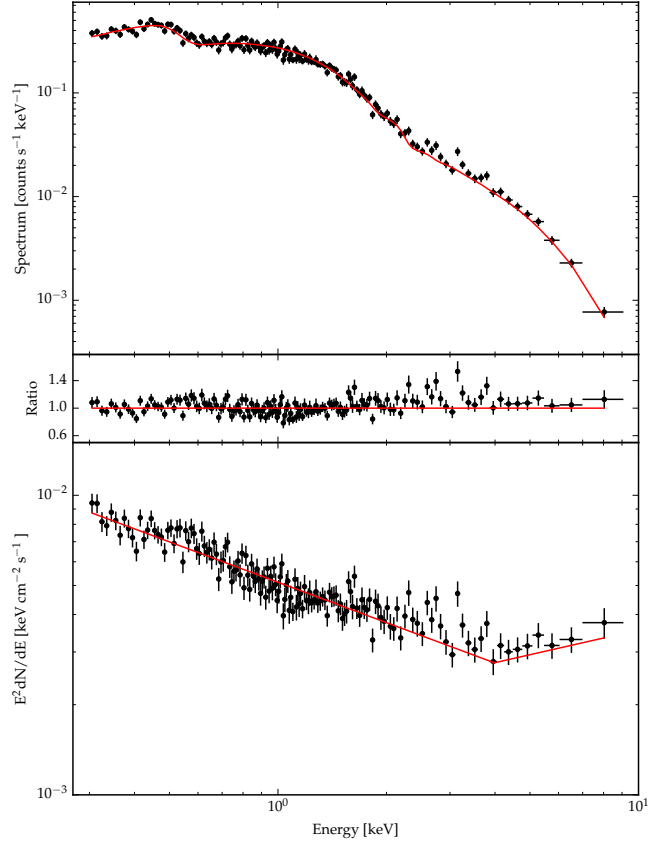


Figure 3. The figure presents spectrum as well as spectral energy distribution of S5 0716+714 including all observations taken during the recent flare in the PC mode. The data are fitted with broken power-law model. The upper panel presents spectral points with fitted model, the middle one shows data and folded-model ratio, while in bottom one the spectral energy distribution is presented. The red line shows the fitted model.

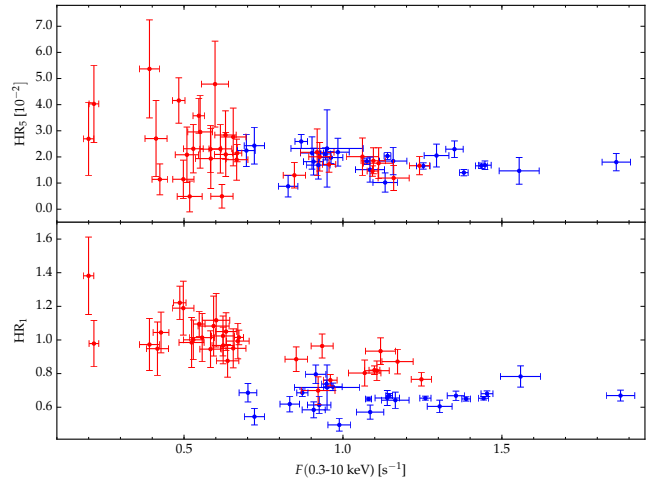


Figure 4. The $HR_5 = F(5-10 \text{ keV})/F(0.3-5 \text{ keV})$ and $HR_1 = F(1-10 \text{ keV})/F(0.3-1 \text{ keV})$ hardness ratios of S5 0716+714 as a function of total source intensity. Observations taken in PC mode and WT mode are marked in red and blue, respectively. One point with large error bars is removed from the second panel for better visibility.